WOOD RESEARCH
62 (6): 2017
983-994

STUDY ON SANDING FORCE, POWER CONSUMPTION AND QUALITY OF CALIBRATING SANDING RECOMBINANT BAMBOO

Bin Luo, Siyu Jin, Feng Cheng, Junhua Ying, Xue Bao, Hongguang Liu, Li Li
Beijing Forestry University, College of Materials Science and Technology
Beijing, P. R. China

(Received July 2017)

ABSTRACT

Recombinant bamboo is a new kind of bamboo-based panel material that has been widely used as a structural material. However, there are many problems in the sanding process of this material. This study analyzes the impacts of sanding parameters on sanding force, sanding active power and sanding efficiency in sanding recombinant bamboo, which is meaningful for improving the sanding quality, reducing power consumption and collocating the sanding parameters more reasonably. Granularity, feed speed, sanding speed and setting sanding thickness have different influences on sanding force, sanding active power and sanding efficiency, and the grey relevancy results show that feed speed has the most significant effect on sanding force, sanding active power and sanding efficiency. The actual sanding thickness is smaller than setting sanding thickness, and the difference between actual and setting values (ΔT_3) is influenced by sanding parameters. Taking a comprehensive consideration of ΔT_3 and standard deviation of actual sanding thickness, determine the optimum schemes according to the method of fuzzy comprehensive evaluation.

KEYWORDS: Recombinant bamboo, sanding, sanding efficiency, sanding force, sanding power consumption.

INTRODUCTION

Bamboo is a good substitute for wood that it takes only 3 to 4 years to grow up. The rational utilization of bamboo can solve the problem of the increasing shortage of timber resources (Shangguan W. 2015). However, the mechanical properties of bamboo do not meet the requirements that most building structures demand because of the hollow structure of bamboo. Recombinant bamboo is a new kind of bamboo-based panel, which can remedy the defects of bamboo. The structural unit of recombinant bamboo is a cross-linked bamboo bundle with a certain fiber direction. After being dried, sized, assembled, and hot pressed, bamboo bundles

are made into recombinant bamboo. The utilization rate of the bamboo in this process is 90%. The tensile strength and compressive strength of recombinant bamboo are 250 MPa and 130 MPa, respectively, which is 2 to 3 times of the common wood. Currently, recombinant bamboo has been widely used as a structural timber in the construction of bridges, houses and outdoor buildings (Baño et al. 2011, Kohler et al. 2013, Shangguan et al. 2014, Zhang et al. 2012).

The high strength and surface hardness of recombinant bamboo cause problems in machining. Especially in the process of calibrating the sanding, surface coke and unequal thickness frequently occur. Presently, there is a few research on sanding recombinant bamboo. Typically, sanding parameters of recombinant bamboo are selected according to the theoretical study of wood sanding or by experienced workers. However, the structures of wood and recombinant bamboo are not exactly the same. Recombinant bamboo and wood can be considered similar in terms of their basic structural unit (bamboo fiber or wood fiber) in the longitudinal direction (Shangguan 2015). The difference between them is that the connection of bamboo fibers is adhesive, and the transverse bonding strength among the bamboo fibers is higher than that of wood (Shangguan et al. 2014). Moreover, the adhesive will soften under high temperatures and then adhere to the cutter body or plug up the chip space, which means that high cutting force and energy consumption are required (Luo et al. 2015). Therefore, the theory of wood sanding is not entirely applicable to the case of recombinant bamboo.

Sanding force is a very important indicator in the study of abrasive belt sanding, which has important influence on sanding quality, sanding efficiency, abrasive loss and energy consumption (Fujiwara et al. 2003). Sanding recombinant bamboo is different from that of steel and other homogeneous materials, as the chip removal forms are more random and the chip shapes are more diverse (Li 2012, Huang et al. 2011). In the sanding process of wood, the sanding force is minimal when the feed speed is vertical to the wood texture direction (transverse sanding), and it reaches a maximum when the sanding is longitudinal. There is a specific texture to the shear failure that occurs with transverse sanding, which is different from the snap texture in longitudinal sanding. The greatest factors affecting the sanding force are granularity and sanding thickness, mainly due to the change in the cutting ratio and the cutting amount per tooth (Luo et al. 2014).

Sanding power generally refers to the average active power applied in the sanding process, it is the overall energy consumption of the sanding system. Changing sanding parameters will cause variation in the energy consumption proportion of each component in the sanding system. The sanding speed has the greatest effect on the sanding power, mainly because increasing the sanding speed will cause the wind resistance to grow sharply. In the sanding process, the ideal state is that the cutting energy consumption takes up a large proportion of energy exerted, and the proportion of mechanical friction, wind resistance and inductive load are kept as low as possible (Luo et al. 2015).

Due to the lack of theoretical research about recombinant bamboo sanding, the sanding energy consumption has generally been high and has not been addressed. This means that sanding quality typically has been poor, and the design of sanding machines has not been improved. This study will analyze the relationship among sanding parameters, including sanding force, sanding power consumption and sanding efficiency. This study aims to provide useful suggestions to improve the processing technology of recombinant bamboo and to perfect sanding theory.

MATERIALS AND METHODS

Materials and facilities

A sanding experimental machine equipped with a reciprocating motion workbench developed at Beijing Forestry University was used in this study, with adjustable sanding thickness accuracy of 0.05 mm. The measuring equipment included a 3D piezoelectric crystal force sensor (KISTLER-3257A, Kistler Instrumente AG, Winterthur, Switzerland), a charge-amplifier (KISTLER-5806, Kistler Instrumente AG, Winterthur, Switzerland), a signal analyzer (NEC Omniace II RA2300, NEC Corporation, Tokyo, Japan), and a multi-function electrical energy meter (TE-PW994H8, Tuoke Intelligent Instrument Co. Ltd., Shanghai, China).

The workpiece was recombinant moso bamboo, with an air-dried density of 1.12 g·cm^{-3}, a surface hardness of 85.79 HD and a size of 150 × 100 × 30 mm, made by Anji Huihuang Bamboo Industry Co. Ltd., Zhejiang, China. Abrasive belts were made by Tianjin Deerfos Co., Ltd. (Tianjin, China) and consisted of twill base material, white fused alumina grit electro coated abrasive, and phenol formaldehyde resin adhesive. The calibrating roller was made of rubber with a spiral pattern and surface hardness was 75 HD, which was made by Haiwei Mechanical Rubber Roller Co. Ltd., Jiangsu, China.

Testing system and methods

As shown in Fig. 1a), the sander was powered by the power supply through a multi-function electrical energy meter, and the sanding active power (*P*) was recorded by this meter. The workpiece was connected with the force sensor, and the force sensor was fixed on the workbench. The sander shut down after sanding one time, and then the workbench was prepared for the next sanding test. The force sensor generated electric signals when forces changed during each sanding process. The signals were amplified by a charge-amplifier, and finally were recorded by a signal analyzer. The relationship between the electric signals and forces (horizontal and vertical directions) had been calibrated before testing. Therefore, the horizontal force (sanding force, *sF*) and vertical force (normal force, *nF*) could be calculated by electric signals. Each test was repeated three times under the same condition for error reduction.

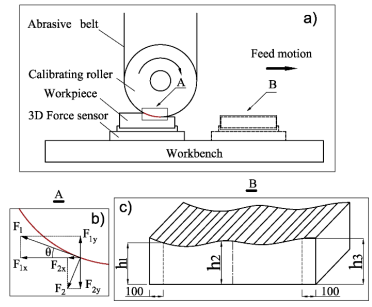

Fig. 1: Testing system.

The forces acting on the workpiece from the abrasive belt were distributed along the contact arc, include sanding tangential force ($\mathbf{F_1}$) and radial force ($\mathbf{F_2}$). The measured *sF* is the resultant force of $\mathbf{F_1}$ and $\mathbf{F_2}$ in the horizontal direction, and *nF* is the resultant force of $\mathbf{F_1}$ and $\mathbf{F_2}$ in the vertical direction, as shown in Fig. 1b).

The consequence of V is much greater than that of U, and θ is extremely small; therefore, the power consumption of the cutting can be estimated by V and sF. Additionally, the sanding efficiency (η) can be calculated according to the following formula:

$$\eta = \frac{sF \times V}{P}$$

The actual sanding thickness along the workpiece surface is different in the sanding process. In order to analyze the relationship between the aTs and the setting sanding thickness (Ts), the aTs is average value of h_1, h_2 and h_3, as shown in Fig. 1c).

Tab. 1 : Experimental factor level.

Factor	Level	Fixed parameter
G	40, 60, 80, 100, 120	U=3.96, V=8.77, Ts=0.2
U	2.52, 2.88, 3.24, 3.60, 3.96, 4.32, 4.68, 5.04, 5.40	G=100, V=8.77, Ts=0.2
V	5.82, 6.58, 7.31, 8.04, 8.77, 9.50, 10.23, 10.96, 11.69	G=100, U=3.96, Ts=0.2
Ts	0.1, 0.2, 0.3, 0.4, 0.5	G=100, U=3.96, V=8.77

G: granularity, *U*: feed speed ($m \cdot min^{-1}$), V: sanding speed ($m \cdot s^{-1}$), Ts: sanding thickness (mm)

The granularity (G), feed speed (U), sanding speed (V) and Ts were the single-variable parameters, and the factor level table was as shown in Tab. 1. The direction of the recombinant bamboo texture was vertical to feed speed during. Each test was repeated three times under the same condition for error reduction.

RESULTS AND DISCUSSION

Vibration source analyze

In the calibration process, the orientation of calibration was opposite to the sF but the same as the nF. Thus, the signal values for computing the sF should be converted into absolute values. The average values of each wave trough (electric signals of the sF) are the signal values of the sF, and for the nF, the signal values are the average values of each wave peak (Fig. 2).

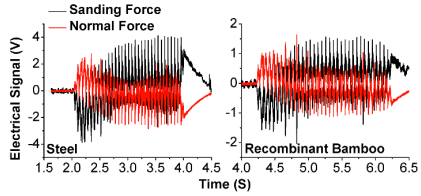

Fig. 2: Electrical signal comparison of sF and nF between steel and recombinant bamboo.

It can be seen that the sF and nF fluctuate continuously during the experiment. This may result from the elasticity of the workpiece, abrasive belt and rubber roller. To determine the main reason for the fluctuations, an experiment was conducted that compared the results between steel and recombinant bamboo in the same sanding conditions. Fig. 2 shows that the forms of the waves are almost unchanged, and the amplitude of the steel sample is larger than that of the recombinant bamboo. This result indicates that the main reasons for the fluctuation were the elasticity of the abrasive belt and rubber roller. Meanwhile, the higher strength of the workpiece resulted higher values for both sF and nF.

Effects of sanding parameters on *sF, nF, P* and *η*

The rake angle of most grits is negative in the sanding process. Therefore, this process can be divided into three states. In the first state, the cutting depth of the grit is small, and the grits rub the workpiece and do not remove material, which causes the surface of the workpiece to deform elastically (Fujiwara et al. 2003). In the second state, with the increased cutting depth, the grits plough through the surface of the workpiece and gullies are created. However, most of the material in the gullies is squeezed to either side of the gullies and forms upthrow, which results in little removal of materials. In the third state, as the cutting depth becomes greater, materials are cut off from the workpiece by the grits (Li 2012). These three states appear simultaneously in the sanding process. In general, friction is smaller than the ploughing and cutting force, and sanding heat occurs mainly due to the friction. The plough force is larger than the cutting force due to the different destructed ways of bamboo fibers. Therefore, the proportion of friction, plough and cutting forces determine the *sF, nF, P* and *η*. The quantity of cutting edges increases and the size of the grits becomes smaller with G increases, which results in the decreased cutting quantity per tooth and cutting ratio, and thus further causes *sF* to decrease. Additionally, as the chip space becomes narrower, the dust discharge from the abrasive belt becomes more difficult and the cutting edges become shorter (block and blunt phenomenon) (Luo et al. 2015, Huang et al. 2011).

Effects of granularity on sF, nF, P and η

According to Fig. 3, *sF, nF, P* and *η* all show the trends of a third power and the nadirs are *G*=60 with *G* increases.

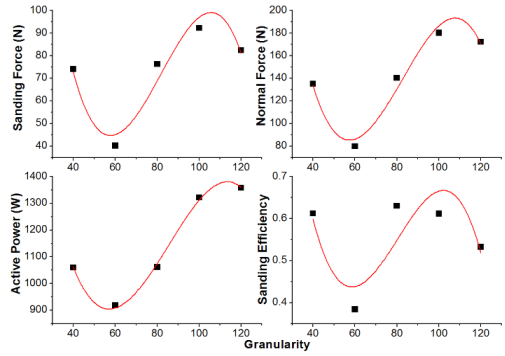

Fig. 3: Effects of granularity on sF, nF, P and η.

The peaks of the forces, *P* and *η* are *G*=100, *G*=120 and *G*=80, respectively. When *G* increased from 40 to 60, the cutting quantity per tooth was reduced and the cutting ratio decreased slightly, which caused a decrease in *sF, nF* and *P*. When *G* increased from 60 to 100, the frictional and plough ratios increased, and the block and blunt phenomenon was more serious, which resulted in increased *sF, nF* and *P*. In the previous studies, the block and blunt phenomenon of medium density fiber board (*MDF*) and particle board (*PB*) usually occurs when *G* is 100 (Luo et al. 2014), while for recombinant bamboo it occurred when *G* was 80. It can be seen from Fig. 4 that the recombinant bamboo fibers were immersed in the adhesive. As a result, it has more adhesive than *MDF* and *PB*. The adhesive was easy to be soft under high temperature and then filled in the chip space that is hard to discharge.

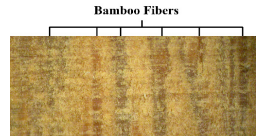

Fig. 4: Partial enlargement figure of recombinant bamboo surface.

This makes the block and blunt phenomenon more possible. When *G* increased from 100 to 120, the friction ratio was extremely high which reduced *sF* and *nF*. Meanwhile, *P* was more sensitive to the friction ratio (sanding heat) and thus *P* increased when *G* increased from 80 to 120. The *η* began to decrease when *G* was 80 and thus causing the sanding heat to increase faster than the sF.

Effects of feed speed on sF, nF, P and η

According to Fig. 5, *sF*, *nF* and *P* increase as *U* increases, and *η* first increases and then decreases.

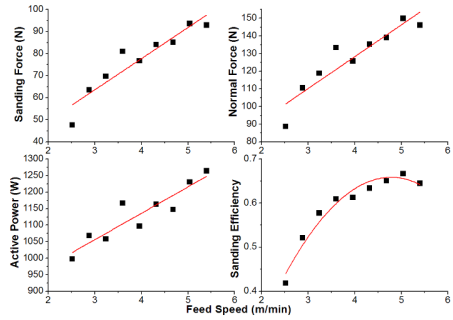

Fig. 5: Effects of feed speed on sF, nF, P and η.

As U increased, the removal of each cutting edge grew when the amount of sanding removal in the unit time increased, which caused an increase in *sF*, *nF* and *P* (Barcik and Samolej 2003, Francisco et al. 2012). When *U* increased from 2.52 to 5.04 m·min^{-1}, the removal capacity of most grits did not achieve the level of saturation. Therefore, the cutting ratio was almost unchanged, while *η* was increased. However, once reaching the saturation level, the frictional ratio would grow due to the block and blunt phenomenon, which resulted in increased sanding heat and decreased *η*.

Effects of sanding speed on sF, nF, P and η

According to Fig. 6, as sanding speed increased, *sF* and *nF* decreased linearly, while *P* increased linearly, but *η* first increased and then decreased. With the increased sanding speed, the removal of each cutting edge decreased, which caused the decreasing *sF* and *nF*.

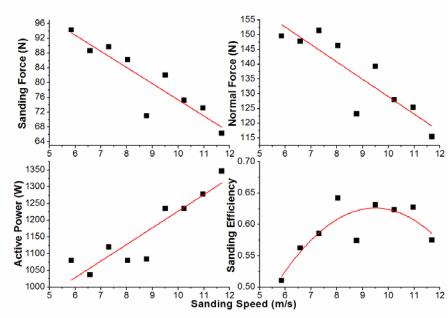

Fig. 6: Effects of sanding speed on sF, nF, P and η.

Furthermore, wind resistance, noise and friction heat between the contact roller and the abrasive belt also increased. The power consumption of the sander was generated by *sF*, electrical loss, mechanical friction and shock, noise and wind resistance. Therefore, *P* is a measure of the comprehensive performance of all the factors. In addition, except for the impact of *sF* and *P,* the inertial effect on *η* should also be noticeable (Barcik and Samolej 2003. Francisco et al. 2012. Liu and Li 2009, Xu et al. 2015, Saloni et al. 2005, Hecker et al. 2007).

Effects of sanding thickness on *sF, nF, P* and *η*

As shown in Fig. 7, with increasing *Ts, sF, nF* and *η* show trends of a second power (*sF* and *nF* reach peaks when *Ts* is 0.4 mm; *η* reaches a peak when *Ts* is 0.3 mm), and *P* shows a linearly increasing trend.

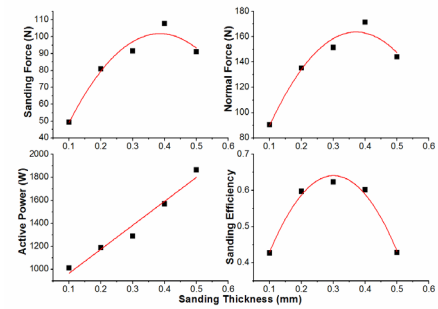

Fig. 7: Effects of sanding thickness on sF, nF, P and η.

The hardness of recombinant bamboo is extremely high, so that *sF* increases sharply as sanding removal increases over the unit time. While *sF* surpasses the maximal friction between the contact roller and the abrasive belt, the abrasive belt would slip on the contact roller and V would decrease. It was found that V was 8.77, 8.75, 8.72, 7.01, 6.22 and 5.43 $mm \cdot s^{-1}$ as Ts was 0.1, 0.2, 0.3, 0.4 and 0.5 mm, respectively. The maximal friction between the contact roller and the abrasive belt was 110 N according to Fig. 3 to Fig. 7. The fixed parameter of *Ts* was set as 0.2 mm in this study due to this phenomenon, which was found in the preliminary experiment. The sanding heat increased rapidly while the abrasive belt slipped, and then the *η* would decrease.

Grey relevancy analysis between sanding parameters and indexes

Traditional mathematical methods of regression analysis, variance analysis and principal component analysis have certain general qualifications, such as the need for large amounts of data, the requirement that the samples must be subject to a typical probability distribution, a linear relationship between the factor data and the system characteristic data, and so on (Liu et al. 2011). These conditions are more difficult to meet during the belt sanding process of the recombinant bamboo due to the anisotropism of the material and the elasticity of the contact roller and abrasive belt The results of the interaction among multiple factors determine the change in *sF, P* and *η*. Grey relevancy analysis is a method that requires only a small amount of data, and it does not require the data to conform to the typical distribution. The basic idea of grey relevancy analysis is to determine relational degrees of sequences according to a similar level of sequential curves. This method is suitable for the analysis of data with high grey degree (data with many uncertain relations) (Chan et al. 2007), and it is also extremely suitable for sanding bamboo material with an abrasive belt. In this study, grey relevancy analysis was used to analyze the correlations between sanding parameters and indexes.

According the results shown in Fig. 8, the correlation between *U* and indexes is the highest. The results of this experiment were slightly different from those of sanding wood material, and the greatest impacts on *sF* and *nF* were *Ts* and *G* during the sanding process.

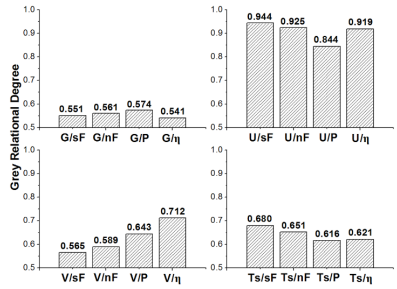

Fig. 8: Grey relational degrees between sanding parameters and indexes.

The unit strength of the recombinant bamboo timber was much greater than that of the wood material, U had effects on impact force and *sF* and *nF* were sensitive to the change of the impact force. At the same time, the change of the impact force caused the momentary slip of the abrasive belt on the contact roller and increased the sanding heat, thus further affecting *P* and *η*. Different *Ts* would result in different cutting quantities per cutting edge, which could also influence *sF* and *nF*.

The V had a great influence on *P* and *η* mainly because of the changes in the wind resistance and friction between the contact roller and the abrasive belt. As a result, it is similar to the experimental results obtained when sanding the wood material (Luo et al. 2015).

Effects of sanding parameters on aTs and optimum scheme of sanding parameters

According to Fig. 9, almost all of *aTs* are less than *Ts* in any sanding conditions, which is the performance of the "elastic grinding" when sanding with abrasive belt. The relations of sanding parameters with *aTs* and *S* (standard deviation of aTs) are not really obvious, except for a significant quadratic relation between *G* and *S*.

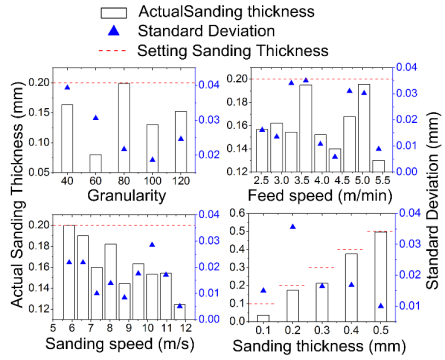

Fig. 9: Effects of sanding parameters on actual sanding thickness.

The smaller difference (ΔTs) between Ts and aTs, the more accurate the sanding calibration is. In addition, the greater S, the worse flatness of the workpiece surface achieve. The quality of the calibrating sanding needs to take both the ΔTs and S into account. Therefore, the fuzzy comprehensive evaluation (*FCE*) method can be used to determine the optimal sanding parameters. Two different groups of weight vector were applied to meet the different processing requirements. It takes (ΔTs, S) = (0.7, 0.3) when taking removal quantity as the primary aim of the processing and (ΔTs, S) = (0.3, 0.7) when taking surface quality as the primary aim on the contrary, the results as shown in Tab. 2.

Tab. 2: Comprehensive optimum scheme of sanding parameters.

Weight vector	(ΔTs, S)=(0.7, 0.3)	(ΔTs, S)=(0.3, 0.7)
Optimum scheme	G=80	G=80,100,120
	U=3.60 m·min^{-1}	U=3.96, 4.32, 5.40 m·min^{-1}
	V=5.82 m·s^{-1}	V=8.77, 11.69 m·s^{-1}
	Ts=0.5 mm	Ts=0.3, 0.4, 0.5 mm

ΔTs: difference between actual and setting sanding thickness;

S: standard deviation of actual sanding thickness;

sF: sanding force (N), nF: normal force (N), P: active power (W), η: sanding efficiency;

G: granularity, U: feed speed (m·min^{-1}), V: sanding speed (m·s^{-1}), Ts: sanding thickness (mm)

As can be seen from the results, the larger mesh size does not necessarily lead to an increase in the accuracy of thickness. The sanding belt with girt size 40 and 60 may remove more workpiece material than grit size 80 (the mesh size of grit size 40 is larger than grit size 80), however, the larger removal quantity does not mean a better precision. In addition, it isn't easy for the sanding belt with grit size 80 to remove the workpiece material, and that makes it difficult to get a better accuracy of thickness. The reasons that U and V need to be slow are explained below. On the one hand, it needs to be ensured that there are enough grits involving in the sanding process. On the other hand, the stability of the rubber roller (the smaller sanding belt speed is, the slighter the rubber roller vibration is) also needs to be ensured. The thicker sanding thickness can guarantee sufficient sanding pressure. Besides, the larger G and V will make a smoother sanding traces, and the more grits involved in the cutting process during unit time is good for improving the surface smoothness. Feeding speed and sanding thickness can be selected as larger as possible under the conditions of certain accuracy of thickness.

Tab. 3: Relations of sanding parameters with sF, nF, P and η.

Equations	R^2
sF	
$sF=-0.996\times10^{-3}\times G^3+0.244\times G^2-18.212\times G+474.777$	0.739
$sF=14.130\times U+21.180$	0.867
$sF=-4.370\times V+119.150$	0.790
$sF=650.198\times Ts^2+500.500\times Ts+5.497$	0.922
nF	
$nF=-1.710\times10^{-3}\times G^3+0.423\times G^2-31.664\times G+833.308$	0.891
$nF=18.000\times U+56.000$	0.841
$nF=-5.884\times V+187.872$	0.735
$nF=1002.424\times Ts2+744.993\times Ts+25.315$	0.923
P	
$P=-5.3\times10-3\times G^3+1.357\times G^2-103.120\times G+3354.898$	0.987
$P=79.873\times U+816.420$	0.832
$P=49.699\times V+730.388$	0.807
$P=2087.204\times Ts+757.941$	0.953
η	
$\eta=-5.575\times10-6\times G^3+1.340\times10-3\times G^2-0.100\times G+2.808$	0.697
$\eta=-0.043U2+0.409\times U-0.318$	0.946
$\eta=-0.008\times V2+0.157\times V-1.118$	0.633
$\eta=-5.260\times Ts^2+3.160\times Ts+0.166$	0.971

sF: sanding force (N), *nF*: normal force (N), *P*: active power (W), *η*: sanding efficiency;
G: granularity, *U*: feed speed ($m\cdot min^{-1}$), V: sanding speed ($m\cdot s^{-1}$), *Ts*: sanding thickness (mm).

Tab. 3 shows a regression analysis of the relationships among four sanding parameters and indexes.

CONCLUSIONS

This study is industrially novel for the process of recombinant bamboo. The relations between sanding parameters and technology indexes are firstly analyzed, and sanding parameters are optimized after considering a variety of technology indexes by fuzzy comprehensive evaluation method. The research results and the experimental method can be used to establish intelligentized process model and rich the database of material process.

(1) The main reasons for the fluctuation are the elasticity of the abrasive belt and rubber roller.
(2) With increasing *G, sF, nF, P* and *η* all show the same trends, firstly decrease then increase and finally decrease. The nadirs are G_{60}, and the peaks of forces, *P* and *η* are G_{100}, G_{120} and G_{80}, respectively. As U increases, *sF, nF* and *P* increase linearly, and *η* first increases and then decreases (the spinodal is U5.04 m/min). As V increases, *sF* and *nF* decrease linearly, P increases linearly, and *η* first increases and then decreases (the spinodal is V9.50 m/s). As *Ts* increases, *sF, nF* and *η* show trends of second power (the peaks of *sF* and *nF* are *Ts* 0.4 mm, the peak of *η* is Ts0.3 mm), and *P* shows a linearly increasing trend.
(3) The grey relation degrees of *U* with *sF, nF, P* and *η* are greater than 0.8. Therefore, different from the sanding of wood material, U influences indexes most.

(4) The optimum schemes of fuzzy comprehensive evaluation for sanding parameters are as follow. When the weight vector (ΔT, S) is (0.7, 0.3), the optimum schemes are G_{80}, $U_{3.60}$ m·min^{-1}, $V_{5.82}$ m·s^{-1}, $Ts_{0.5}$ mm, respectively; when (ΔT, S) is (0.3, 0.7), the optimum schemes are $G_{80,100,120}$, $U_{3.96,\ 4.32,\ 5.40}$ m·min^{-1}, $V_{8.77,\ 11.69}$ m·s^{-1} , $Ts_{0.3,\ 0.4,\ 0.5}$ mm, respectively.

ACKNOWLEDGEMENTS

This work was supported by the science and technology innovation plan of Beijing forestry university (BLX2015-19)

REFERENCES

1. Baño V., Arriaga F., Soilán A., Guaita M., 2011: Prediction of bending load capacity of timber beams using a finite element method simulation of knots and grain deviation, Biosystems Engineering 109: 241-249.
2. Barcik S., Samolej A., 2003: Experimental investigation of sanding process on disc sander, Wood Res 48: 36-42.
3. Chan J., W. K., Tong T., K.L., 2007: Multi-criteria material selections and end-of-life product strategy: grey relational analysis approach, Materials & Design 28: 1539-1546.
4. Francisco M. F., Manoel C., Marcos T. T. G., 2012: Influence of belt speed, grit sizes and pressure on the sanding of *Eucalyptus grandis* wood, Cerne Lavras 18: 231-237.
5. Fujiwara Y., Fujii Y., Okumura S., 2003: Effect of removal of deep valleys on the evaluation of machined surface of wood, For Prod J 53: 58–62.
6. Hecker R. L., Liang S. Y., Wu X. J., Xia P., Jin D. G. W., 2007: Grinding force and power modeling based on chip thickness analysis, Int J Adv Manuf Technol 33: 449-459.
7. Huang Y., Yang C. Q., Huang Z., 2011: Experimental research on abrasive belt grinding for 304 stainless steel, China Mech Eng 22: 291-295.
8. Kohler J., Brandner R., Thiel A. B., Schickhofer G., 2013: Probabilistic characterisation of the length effect for parallel to the grain tensile strength of Central European spruce, Engineering Structures 56: 691-697.
9. Liu B., Li L., 2009: Sanding force of wood and medium-density fiberboard, Journal of Beijing Forestry University 31:197-201.
10. Li L., 2012: Wood cutting theory and tools. China Forestry Press. Beijing.
11. Liu S. F., Dang Y. G., Fang .Z G., Xie N. M., 2011: Grey system theory and apply, Science press. Beijing.
12. Luo B., Li L., Liu H. G., Wang M. Z., Xu M. J., 2015: Effects of sanding parameters on sanding force and normal force in sanding wood-based panels, Holzforschung 69: 241-245.
13. Luo B., Li L., Liu H. G., Xu M. J., Xing F. R., 2014: Analysis of sanding parameters, sanding force, normal force, power consumption, and surface roughness in sanding wood-based panels, BioResources 9: 7494-7503.
14. Saloni D. E., Lemaster R. L., Jackson S. D., 2005: Abrasive machining process characterization on material removal rate, final surface texture, and power consumption for wood, For Prod J 55: 35-52.
15. Shangguan W., 2015: Research on physical and mechanical properties of bamboo scrimber. Chinese Academy of Forestry, Beijing, China, 16 pp.

16. Shangguan W., Zhong Y., Xing X., Zhao R., Ren H., 2014: 2D model of strength parameter for bamboo scrimber, Bioresources 9: 7073-7085.
17. Xu M. J., Li L., Luo B., Xing F. R., 2015: Study on sanding force and sanding optimal parameters of Manchurian ash, European Journal of Wood and Wood Products 73: 385-393.
18. Zhang J. Z., Ren H. Q., Zhong Y., Zhao R., 2012: Analysis of compressive and tensile mechanical properties of recombinant bamboo, Journal of Nanjing Forestry University (natural science edition) 36: 107-111.

Bin Luo*, Siyu Jin, Feng Cheng, Junhua Ying, Xue Bao, Hongguang Liu, Li Lii
Beijing Forestry University
College of Materials Science and Technology
No.35 Tsinghua East Rd)
Haidian District
Beijing, 100083
P. R. China
*Corresponding authors: luobin_731@126.com